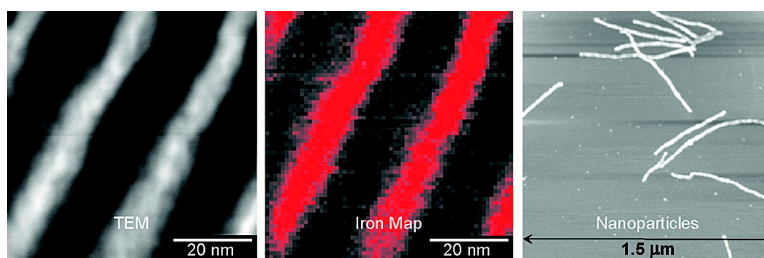Communication

Self-Assembly Approach toward Magnetic Silica-Type Nanoparticles of Different Shapes from Reverse Block Copolymer Mesophases

Carlos B. W. Garcia, Yuanming Zhang, Surbhi Mahajan, Francis DiSalvo, and Ulrich Wiesner

More About This Article

Additional resources and features associated with this article are available within the HTML version:

- Supporting Information
- Links to the 5 articles that cite this article, as of the time of this article download
- Access to high resolution figures
- Links to articles and content related to this article
- Copyright permission to reproduce figures and/or text from this article

View the Full Text HTML

Self-Assembly Approach toward Magnetic Silica-Type Nanoparticles of Different Shapes from Reverse Block Copolymer Mesophases

Carlos B. W. Garcia, Yuanming Zhang, Surbhi Mahajan, Francis DiSalvo,§ and Ulrich Wiesner*

Department of Materials Science and Engineering and Department of Chemistry and Chemical Biology, Cornell University, Bard Hall, Ithaca New York 14853

Received July 7, 2003; E-mail: ubw1@cornell.edu

The synthesis of nanoparticles from reverse block copolymer mesophases is an effective route to controlling both the size distributions of the nanoparticles and their shape. Particles on this length scale may find use in biological systems providing means for labeling of biomolecules for single particle tracking or separation and drug delivery.[1] For catalysis, these materials may become important based on their size and high surface area content. Adding magnetic properties to the particles could lead to a controlled drug delivery system where potentially harmful compounds could be localized around the area of infection with the use of magnetic fields, e.g. in cancer treatment.[2,3] Although several other methods to generate nanoparticles are available, these systems are generally limited to spherical geometries with broad size distributions.[4–6] Here we show that using block copolymers with narrow size distributions to structure iron oxide−aluminosilicate ceramic materials on nanometer-length scales may supply a versatile approach to controlling each one of the parameters of size, shape, and magnetic properties separately.

Nanostructuring inorganic systems with amphiphilic block copolymers is an exciting area of research.[7–9] The resulting polymer−inorganic hybrids offer enormous scientific and technological promise in areas ranging from microelectronics to nanobiotechnology.[10] Thus far, only a few reports have been made investigating the ability of block copolymers to structure silica-based materials into the "reverse" mesophases known to block copolymer systems, namely the spherical and cylinder structures where the inorganic material is the minority phase. Ulrich et al. demonstrated the ability of the amphiphilic block copolymer poly-(isoprene−b-ethylene oxide), PI−b-PEO, to structure silica precursors into these reverse mesophases, which upon dissolution of the organic matrix led to well-defined silica nanoparticles of spheres, cylinders, and plates based on the original structure of the mesophase prepared.[11] Brinker et al. also observed these reverse mesophases using a different polymer/silica system.[12] Here we describe a self-assembly approach toward functional, i.e., magnetic, nanoparticles in the shape of spheres, plates, and lamellae.

The block copolymer PI−b-PEO was synthesized using anionic polymerization from a technique described elsewhere.[13] Three polymers were made with molecular weights of 22 700 g/mol (P1), 16 200 g/mol (P2), and 22 900 g/mol (P3) with PEO weight fractions of 0.134, 0.125, and 0.161, respectively. Each polymer had a narrow molecular weight distribution with a polydispersity index ≤1.05. Polymer−inorganic composites were made by forming a solution of PI−b-PEO in a 50−50 mixture of dry tetrahydrofuran and chloroform with iron (III) ethoxide powder. In a second vial, a sol of 3-(glycidyloxypropyl) trimethoxysilane (GLYMO) and aluminum *sec*-butoxide was prepared using a procedure described previously.[8] Varying amounts of the sol were added to the polymer−iron ethoxide solution in different experiments. After
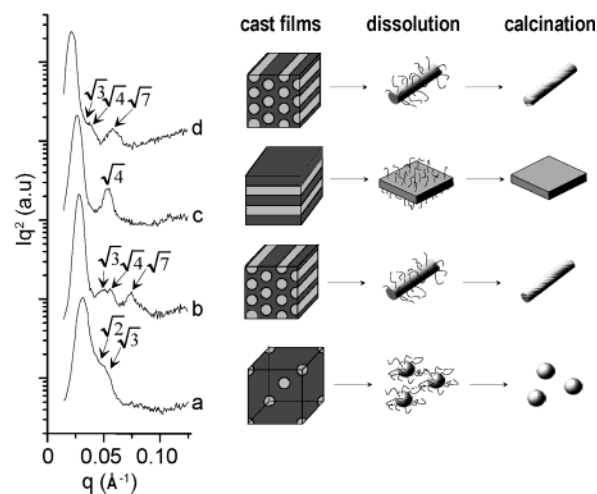

Figure 1. SAXS traces of the polymer−inorganic composite films and mesophase assignment: (a) P1C25, (b) P2C30, (c) P2C25, and (d) P3C50. The schematic at the right shows nanoparticle shapes obtained from each phase through dissolution of the films and subsequent calcination.

stirring the combined solutions for an hour, films were cast by evaporation of the solvent, causing the polymer and inorganic constituents to co-assemble into the different mesophases, depending on the ratio of inorganic material to polymer.

Four composite films were made with different iron loadings and sol content designated as P1C25 (25 mol % Fe on a cation basis), P2C30 (30 mol % Fe), P2C25 (25 mol % Fe), and P3C50 (50 mol % Fe) to generate the three different mesophases shown in Figure 1. Small-angle X-ray scattering (SAXS) experiments were performed on a Bruker-AXS Nanostar (Cu Kα, 1.54 Å) operated at 40 kV, 40 mA in transmission. The SAXS traces in Figure 1 are consistent for materials with sphere (P1C25, a), hexagonal cylinder (P2C30, b and P2C50, d), and lamellar morphologies (P2C25, c) and show that successful nanostructure formation is achieved up to 50% iron loadings on a cation basis. After the films were cast, they were annealed in a vacuum oven at 130 °C for 1 h to remove any volatile byproducts of the reaction. The weight ratio of inorganic material to polymer after removal of volatile byproducts was 0.404 for P1C25, 0.482 for P2C30, 0.632 for P2C25, and 0.496 for P3C50.

Transmission electron microscopy was performed on a JEOL 1200EX operating at 120 keV to corroborate all morphology assignments from SAXS. Figure 2a shows a bright field image of the local structure of sample P2C30. The image depicts a hexagonal cylinder array with the dark areas in the image corresponding to the more electron-dense iron−aluminosilicate cylinders. For the same sample, a VG HB-501UX dedicated scanning transmission electron microscope (STEM) operating at 100 keV with a cold-field emission source was used to acquire an annular dark-field image (Figure 2b, resolution ~0.2 nm). A single-crystal YAP
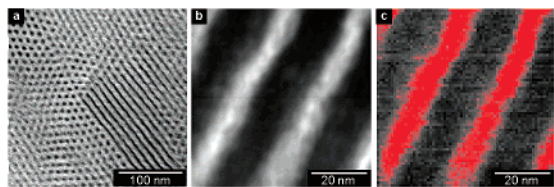
§ Cornell University, Baker Laboratory.

Figure 2. (a) Bright-field TEM micrograph of sample P2C30 microtomed from the cast film showing a grain boundary between cylinders head-on and on their side. (b) Dark-field STEM image of the same sample and (c) corresponding EELS iron map showing a homogeneous distribution of iron (shown in red). Note that in (a) and (b) contrasts are inverted.
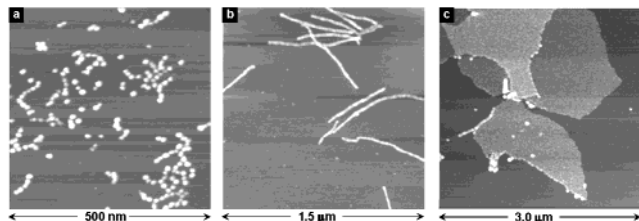

Figure 3. SFM images of the heat treated spheres (a), cylinders (b), and plates (c) on mica.

scintillator/PMT combination was used for serial electron energy loss spectroscopy (EELS) and energy filtered imaging to show the presence and location of the iron in the film indicated by red in Figure 2c. The image clearly shows a homogeneous distribution of iron in the region of the aluminosilicate cylinder domains.

Solutions of dispersed nanoparticles with different shape and size were generated by dissolution and ultrasonication of the composite films in toluene (0.01 wt % solution). From studies of similar systems a layer of polyisoprene is expected to surround the iron—aluminosilicate particles, stabilizing them in the organic solvent, while the PEO block remains embedded in the inorganic matrix.[11,14] Freshly cleaved mica was dip-coated in the solutions. Subsequent calcination at 550 °C burned away all organic constituents. This treatment is also expected to nucleate and grow iron oxide precipitates within the aluminosilicate particles. Scanning force microscopy (SFM) was performed on a Digital Instruments Multimode SPM under tapping mode to characterize these mica surfaces. Figure 3 shows individual nanoparticles originating from the sphere, cylinder, and lamellar morphologies.

In studies of samples with the inverse hexagonal cylinder morphology (inorganic matrix with polymer cylinders) we have established that calcination of the present composites at temperatures of 550 °C and above leads to superparamagnetic mesoporous materials with nanometer-sized crystalline γ-Fe$_2$O$_3$ particles embedded in the walls.[15] Thus, high-temperature treatment of the present nanoparticles is also expected to lead to magnetic ceramics. However, at the level of individual nanoparticles it is very difficult to demonstrate that γ-Fe$_2$O$_3$ has been formed and that the particles are superparamagnetic. We therefore took an alternative approach. Rather than the individual nanoparticles, the respective bulk composites were calcined, leading to an expected collapse of the polymer matrix sintering the individual ceramic nanodomains together. Long heat treatments lead to the growth of larger iron oxide particles ($\sim$50 nm) that can be structurally as well as magnetically characterized. Using a Scintag $\theta-\theta$ diffractometer (Cu Kα) the crystalline phase identified in sample P3C50 was indeed the ferrimagnetic γ-Fe$_2$O$_3$ phase (Figure 4a). For the same sample, the magnetic properties were measured using a Quantum Design MPMS SQUID magnetometer at 300 K (Figure 4b). A slight
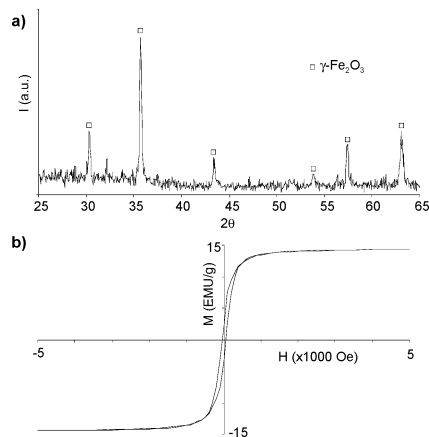

Figure 4. (a) XRD of the P3C50 bulk film calcined to 550 °C showing predominantly a γ-Fe$_2$O$_3$ crystalline phase. (b) Magnetization (M) versus field (H) curves for the same sample measured at 300 K.

hysteresis in the magnetization curve indicates that either the particles are multidomain or that moments between individual particles are interacting.

The synthesis of iron oxide—aluminosilicate nanoparticles from reverse block copolymer mesophases is an effective route to controlling both the size distributions of the nanoparticles and their shape.[10] By simply increasing the amount of inorganic material added, spheres, cylinders, and lamellae are formed. Calcination of these materials propagates the nucleation and growth of a magnetically active γ-Fe$_2$O$_3$ crystalline phase within the amorphous aluminosilicate matrix. These results pave the way to magnetic nanoparticles where the size, shape, and iron oxide concentration can be controlled leading to tunable magnetic and optical properties of nanostructures on surfaces and interesting research in catalysis, molecular labeling, and detection as well as controlled drug delivery using external magnetic fields.

References

(1) Saxton, M. J.; Jacobson, K. *Annu. Rev. Biophys. Biomol. Struct.* **1997**, *26*, 373.
(2) Liu, C.; Zou, B.; Rondinone, A. J.; Zhang, Z. J. *J. Phys. Chem. B* **2000**, *104*, 1141.
(3) Brigger, I.; Dubernet, C.; Couvreur, P. *Adv. Drug Del. Rev.* **2002**, *54*, 631.
(4) Liu, Y.; Pinnavaia, T. J. *J. Am. Chem. Soc.* **2003**, *125*, 2376.
(5) Ono, K.; Okuda, R.; Ishii, Y.; Kamimura, S.; Oshima, M. *J. Phys. Chem. B* **2003**, *107*, 1941.
(6) Landfester, K. *Adv. Mater.* **2001**, *13*, 765.
(7) Bagshaw, S. A.; Prouzet, E.; Pinnavaia, T. J. *Science* **1995**, *269*, 1242.
(8) Templin, M.; Franck, A.; Du Chesne, A.; Leist, H.; Zhang, Y.; Ulrich, R.; Schädler, V.; Wiesner, U. *Science* **1997**, *278*, 1795.
(9) Zhao, D.; Feng, J.; Huo, Q.; Melosh, N.; Fredrickson, G. H.; Chmelka, B. F.; Stucky, G. D. *Science* **1998**, *279*, 548.
(10) Simon, P. F. W.; Ulrich, R.; Spiess, H. W.; Wiesner, U. *Chem. Mater.* **2001**, *13*, 3464.
(11) Ulrich, R.; Du Chesne, A.; Templin, M.; Wiesner, U. *Adv. Mater.* **1999**, *11*, 141.
(12) Yu, K.; Hurd, A. J.; Eisenberg, A.; Brinker, C. J. *Langmuir* **2001**, *17*, 7961.
(13) Allgaier, J.; Poppe, A.; Willner, L.; Richter, D. *Macromolecules* **1997**, *30*, 1582.
(14) De Paul, S. M.; Zwanziger, J. W.; Ulrich, R.; Wiesner, U.; Spiess, H. W. *J. Am. Chem. Soc.* **1999**, *121*, 5727.
(15) Garcia, C. B. W.; Zhang, Y.; DiSalvo, F.; Wiesner, U. *Angew. Chem., Int. Ed.* **2003**, *42*, 1526−1530.

JA037116Q